0026-895X/06/7004-1255–1263$20.00
MOLECULAR PHARMACOLOGY
Copyright © 2006 The American Society for Pharmacology and Experimental Therapeutics
Mol Pharmacol 70:1255–1263, 2006

Vol. 70, No. 4
26815/3143634
Printed in U.S.A.

Role in the Selectivity of Neonicotinoids of Insect-Specific Basic Residues in Loop D of the Nicotinic Acetylcholine Receptor Agonist Binding Site

Masaru Shimomura, Maiko Yokota, Makoto Ihara, Miki Akamatsu, David B. Sattelle, and Kazuhiko Matsuda

Department of Applied Biological Chemistry, School of Agriculture, Kinki University, Nara, Japan (M.S., M.Y., M.I., K.M.); Graduate School of Agriculture, Kyoto University, Kyoto, Japan (M.A.); MRC Functional Genetics Unit, Department of Physiology, Anatomy and Genetics, Le Gros Clark Building, University of Oxford, Oxford, United Kingdom (D.B.S.)

Received May 18, 2006; accepted July 25, 2006

ABSTRACT

The insecticide imidacloprid and structurally related neonicotinoids act selectively on insect nicotinic acetylcholine receptors (nAChRs). To investigate the mechanism of neonicotinoid selectivity, we have examined the effects of mutations to basic amino acid residues in loop D of the nAChR acetylcholine (ACh) binding site on the interactions with imidacloprid. The receptors investigated are the recombinant chicken $\alpha4\beta2$ nAChR and *Drosophila melanogaster* D$\alpha2$/chicken $\beta2$ hybrid nAChR expressed in *Xenopus laevis* oocytes. Although mutations of Thr77 in loop D of the $\beta2$ subunit resulted in a barely detectable effect on the imidacloprid concentration-response curve for the $\alpha4\beta2$ nAChR, T77R;E79V double mutations shifted the curve dramatically to higher affinity binding of imidacloprid. Likewise, T77K;E79R and T77N;E79R double mutations in the D$\alpha2\beta2$ nAChR also resulted in a shift to a higher affinity for imidacloprid, which exceeded that observed for a single mutation of Thr77 to basic residues. By contrast, these double mutations scarcely influenced the ACh concentration-response curve, suggesting selective interactions with imidacloprid of the newly introduced basic residues. Computational, homology models of the agonist binding domain of the wild-type and mutant $\alpha4\beta2$ and D$\alpha2\beta2$ nAChRs with imidacloprid bound were generated based on the crystal structures of acetylcholine binding proteins of *Lymnaea stagnalis* and *Aplysia californica*. The models indicate that the nitro group of imidacloprid interacts directly with the introduced basic residues at position 77, whereas those at position 79 either prevent or permit such interactions depending on their electrostatic properties, thereby explaining the observed functional changes resulting from site-directed mutagenesis.

Nicotinic acetylcholine receptors (nAChRs) play a central role in rapid cholinergic synaptic transmission (Sattelle, 1980; Sattelle and Breer, 1990) and are important targets of insecticides (Gepner et al., 1978; Matsuda et al., 2001, 2005). Of the insecticides acting on insect nAChRs, imidacloprid and its analogs (Fig. 1), referred to as neonicotinoids, are used worldwide as agrochemicals (Matsuda et al., 2001, 2005; Tomizawa and Casida, 2005). In addition, neonicotinoids are employed in animal health as flea repellants (Mencke and Jeschke, 2002; Rust, 2005). Most neonicotinoids are partial agonists of native (Nagata et al., 1996; Deglise et al., 2002; Ihara et al., 2006) and recombinant (Shimomura et al., 2002, 2003, 2004; Ihara et al., 2003, 2004; Matsuda et al., 1998, 2005) nAChRs, but some antagonize the acetylcholine-induced responses of native insect neurons (Salgado and Saar, 2004; Ihara et al., 2006) and others show superagonist actions (Ihara et al., 2004).

Neonicotinoids act selectively on insect nAChRs, accounting at least in part for the selective toxicity to insects over vertebrates (Matsuda et al., 2001, 2005; Tomizawa et al., 2003; Tomizawa and Casida, 2005). Neonicotinoids possess either a nitro or a cyano group; these groups have been postulated to contribute directly to their selectivity (Matsuda et al., 2001, 2005; Tomizawa et al., 2003; Tomizawa and Casida, 2005). The molecular targets of neonicotinoids are nAChRs, which belong to the Cys-loop family of ligand-gated ion channels and usually consist of α and non-α subunits (Corringer et al., 2000; Karlin, 2002; Lindstrom, 2003). How-

M.S. and K.M. were supported by the Program for Promotion for Basic Research Activities for Innovative Biosciences (Bio-oriented Technology Research Advancement Institution, BRAIN). D.B.S. was supported by the Medical Research Council of the UK.

Article, publication date, and citation information can be found at http://molpharm.aspetjournals.org.

doi:10.1124/mol.106.026815.

ABBREVIATIONS: ACh, acetylcholine; nAChR, nicotinic acetylcholine receptor; PCR, polymerase chain reaction; SOS, standard oocyte saline; PDFAMS, Protein Discovery Full Automatic Modeling System; AChBP, acetylcholine binding protein; PDB, Protein Data Bank.

ever, α7, α8, and α9 subunits each form functional homomers when expressed in *Xenopus laevis* oocytes (Couturier et al., 1990; Elgoyhen et al., 1994; Gerzanich et al., 1994), although α7 (Palma et al., 1999; Azam et al., 2003) and α9 (Elgoyhen et al., 2001) subunits can coassemble with other subunits, resulting in characteristics distinct from those of homomers.

The binding site for ACh and other agonists is formed by six loops, A–F, in the extracellular, N-terminal domain. Loops A–C are confined to α subunits, whereas loops D–F are present either in non-α subunits of α/non-α heteromers or in the α subunits of homomers (Corringer et al., 2000) and α/α heteromers (e.g., α9/α10) (Elgoyhen et al., 2001).

We have shown previously that when the nitro group of imidacloprid interacts with basic residues, the nitrogen atoms in the imidazolidine ring of imidacloprid become positive, thereby strengthening cation-π interactions with tryptophan residues in loop B (Matsuda et al., 2001, 2005). This "induced-fit" mechanism can also account for the selective actions of other neonicotinoids such as thiacloprid and acetamiprid, both of which possess a cyano group. Consistent with this view, we have found that Q79R and Q79K mutations in loop D of chicken α7 homomer enhance the peak current amplitude of the currents recorded from the expressed receptor in response to imidacloprid and nitenpyram (Shimomura et al., 2002). Because most insect nAChR non-α subunits possess basic residues in loop D at the position corresponding to Gln79 (residue numbering is from the start methionine) of the α7 subunit (Table 1), it was postulated that such basic residues are likely to contribute to the selective neonicotinoid actions on insect nAChR. Nevertheless, although significant, the shift in the neonicotinoid concentration-response curves resulting from the Q79R and Q79K mutations in the α7 nAChR was small (Shimomura et al., 2002) and insufficient to account for neonicotinoid selectivity. In addition, it is possible that changes in the responses to neonicotinoids resulting from the addition of basic residues to loop D may be limited to the homomeric α7 nAChRs.

In the present study, two-electrode voltage-clamp electrophysiology has been employed to investigate the effects on the responses to imidacloprid of chicken α4β2 and *Drosophila melanogaster* Dα2/chicken β2 hybrid nAChRs of mutating Thr77 and Glu79 in the β2 subunit to basic amino acid residues. These residues correspond to Gln79 and Tyr81 of the α7 nAChR (see Table 1). To assist in interpreting the results from mutagenesis experiments, three-dimensional models for the agonist binding site of the nAChRs with imidacloprid docked have been constructed based on the crystal structures of acetylcholine binding proteins (AChBPs), with either nicotine (Celie et al., 2004) or epibatidine (Hansen et al., 2005) bound, both of which share the pyridine ring with imidacloprid. The models indicate that not only basic residues but also neighboring structural features are involved in the selectivity of nAChR-imidacloprid interactions.

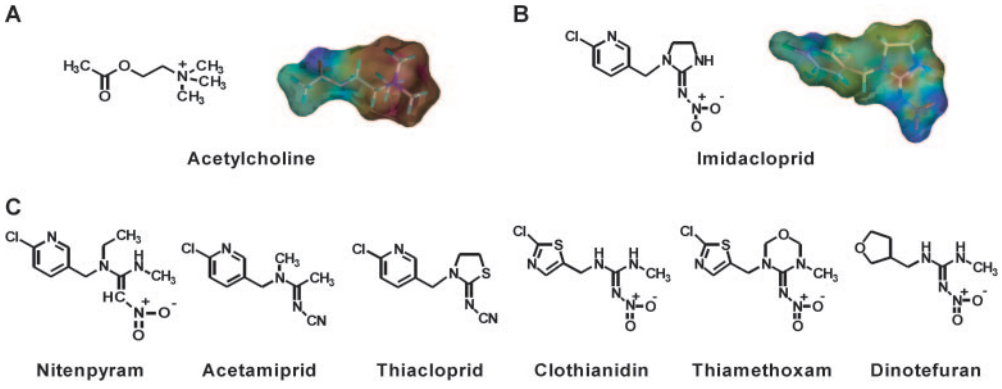

Fig. 1. Chemical structures and electrostatic potential maps of acetylcholine (A) and imidacloprid (B). The electrostatic potentials were calculated by the MNDO, semiempirical, molecular orbital method. Positive and negative potentials are shown in red and blue, respectively. C, neonicotinoid insecticides which have been developed after the discovery of imidacloprid.

TABLE 1
Alignment of amino acid sequence in loop D of the ACh binding site of vertebrate and insect nicotinic acetylcholine receptors

Subunits	Amino Acid Number of Chicken β2 Subunit[a]									
	73	74	75	76	77	78	79	80	81	82
Vertebrates										
Chicken α7	N	I	W	L	Q	M	Y	W	T	D
Chicken β2	N	V	W	L	T	Q	E	W	E	D
Chicken β4	N	V	W	L	N	Q	E	W	I	D
Human β2	N	V	W	L	T	Q	E	W	E	D
Human β4	N	V	W	L	K	Q	E	W	T	D
Human δ	N	V	W	I	E	H	G	W	T	D
Human ϵ	S	V	W	I	G	I	D	W	Q	D
Rat β1	K	V	Y	L	D	L	E	W	T	D
Rat β2	N	V	W	L	T	Q	E	W	E	D
Rat β4	S	I	W	L	K	Q	E	W	T	D
Insects										
Fruit fly Dβ1	N	V	W	L	R	L	V	W	Y	D
Fruit fly Dβ2	N	L	W	V	K	Q	R	W	F	D
Fruit fly Dβ3	H	C	W	L	N	L	R	W	R	D
Locusta migratoria β	N	V	W	L	R	L	V	W	N	D
Myzus persicae β1	N	V	W	L	R	L	V	W	R	D
Heliothis virescens β1	N	V	W	L	R	L	V	W	M	D

[a] Residue numbering is from the start methionine.

Materials and Methods

Preparation of DNAs Encoding Mutant β2 Subunits. The chicken nAChR β2 subunit cDNA in the pcDNA3.1 vector (Invitrogen, Carlsbad, CA) was used as a template for mutagenesis (Swick et al., 1992; Bertrand et al., 1994). Mutations were introduced by PCR as described previously (Matsuda et al., 2000; Shimomura et al., 2002). Oligonucleotides T77N sense and T77N antisense were prepared to generate the β2 T77N mutation in the β2 subunit. The T7 primer (5′-TAATACGACTCACTATAGGGAGACCC-3′) and β2 antisense primer (5′-CTTCATTGCAGACCACATGC-3′) were designed, respectively, on the basis of the sequence flanking the multiple cloning site of the pcDNA3.1 vector and the β2 cDNA approximately 1.3 kilobase pairs downstream of the start methionine codon. The first round PCR was carried out using 1 U of KOD-Plus polymerase (Toyobo, Shiga, Japan), 100 ng of wild-type pcDNA3.1-β2 as template, 0.3 μM primers (T7 primer and T77K antisense; β2 antisense and T77K sense), and 0.2 mM dNTP mixture in a 50-μl solution for 30 cycles of 94°C for 15 s, 45°C for 30 s, and 68°C for 60 s. The second-round PCR was conducted using 1 U of KOD-Plus, 20 ng each of the first round PCR products and 0.3 μM primers (T7 primer and β2 antisense), and 0.2 mM dNTP mixture in a 50-μl solution for 30 cycles of 94°C for 15 s, 48°C for 30 s, and 68°C for 90 s, yielding a single DNA band. After purification using a low melting-point agarose gel (Promega, Madison, WI), the isolated PCR fragment was digested using BamHI (Takara, Shiga, Japan) and subcloned into pcDNA3.1-β2. This plasmid was cut with BamHI and ligated with a 1.3-kilobase pair BamHI fragment of pcDNA3.1-β2 to complete the full-length mutant β2 subunits. Other DNA constructs encoding the T77N, T77R, E79R, E79V, T77K;E79R, T77N;E79R and T77R;E79V mutants were prepared in a similar manner.

Preparation and Nuclear Injection of *X. laevis* Oocytes. Mature *X. laevis* female frogs were anesthetized by immersion in 1.5 g/l tricaine for 30 to 45 min, depending on body weight, before removal of a part of the ovary. We made as much effort as possible to minimize animal suffering and reduce the number of animals used. Oocytes at stage V or VI of development were separated from the follicle cell layer after treatment with 2 mg/ml collagenase (type IA; Sigma, St. Louis, MO). The nucleus of each defolliculated oocyte was injected with 20 nl of cDNA in distilled water (0.1 ng/nl) and incubated at 18°C in standard oocyte saline (SOS; 100 mM NaCl, 2.0 mM KCl, 1.8 mM $CaCl_2$, 1.0 mM $MgCl_2$, and 5.0 mM HEPES, pH 7.6), supplemented with 100 units/ml penicillin, 100 μg/ml streptomycin, 50 μg/ml gentamicin, and 2.5 mM sodium pyruvate. Electrophysiology was performed 3 to 6 days after nuclear injection.

Electrophysiology. *X. laevis* oocytes were secured in a recording chamber that was perfused (7–10 ml/min) continuously with SOS, containing 0.5 μM atropine to eliminate any responses resulting from activation of endogenous muscarinic AChRs, using a gravity-fed delivery system described previously (Matsuda et al., 1998; Shimomura et al., 2004b). Membrane currents were recorded using 2.0 M KCl-filled electrodes (resistances, 0.5–5.0 MΩ) linked to a GeneClamp 500B (Molecular Devices, Sunnyvale, CA) amplifier. The oocyte membrane was clamped at −100 mV. Currents were displayed using a pen recorder.

To prepare test solutions, stock solutions of ligands were diluted with SOS containing 0.5 μM atropine, whereas those containing ACh in SOS were prepared immediately before experiments. Stock solutions of imidacloprid (300 mM) were prepared in dimethyl sulfoxide and diluted with SOS before tests. Dimethyl sulfoxide at concentrations lower than 1% (v/v) had no effect on the responses (Matsuda et al., 1998). Concentration-response data were obtained by challenging oocytes at intervals of 3 to 5 min with increasing concentrations of an agonist. The peak amplitude of the current recorded in response to each challenge was normalized to the maximum amplitude of the response to ACh. For example, data from the wild-type chicken α4β2 and *D. melanogaster* Dα2/chicken β2 hybrid nAChRs as well as those from the T77N, T77R, E79R, E79V and T77N;E79R mutants of Dα2β2 nAChR were normalized to the response to 100 μM ACh; data from the T77K, T77N, T77R, T77K;E79R, T77N;E79R and T77R;79V mutants of the α4β2 nAChR, and T77K and T77R;E79V mutants of the Dα2β2 nAChR were normalized to the response to 300 μM ACh; data from the E79R and E79V mutants of the α4β2 nAChR and the T77K;E79R mutant of the Dα2β2 nAChR were normalized to the response to 1 mM ACh.

Using Prism software (GraphPad Software, San Diego, CA), a nonlinear regression analysis was applied to normalize data enabling determination of I_{max}, the maximum normalized response, EC_{50}, the concentration (M) giving half the maximum normalized response, and n_H, the Hill coefficient (Matsuda et al., 1998; Shimomura et al., 2002). Experiments were conducted at room temperature (19–25°C). Imidacloprid was synthesized as described previously (Moriya et al., 1992). ACh chloride and atropine sulfate were purchased from Sigma Aldrich Japan (Tokyo, Japan).

Receptor Modeling. Modeling of the N-terminal domain of chicken α4β2 and *D. melanogaster* Dα2/chicken β2 hybrid nAChRs was carried out using the molecular modeling software package Sybyl (ver. 6.91; Tripos Associates, Inc., St. Louis, MO) and the homology modeling software Protein Discovery Full Automatic Modeling System Pro (PDFAMS ver. 2.0; In-Silico Sciences, Inc., Tokyo, Japan), originally developed by Ogata and Umeyama (2000). Models of the α4β2 nAChR with imidacloprid bound were constructed using PDFAMS ligand and complex mode. First, using PDFAMS, primary sequences of α4 and β2 nAChR subunits obtained from the ligand-gated ion channel database (http://www.ebi.ac.uk/compneur-srv/LGICdb/cys-loop.php) were automatically aligned with homologous sequences in the FAMS database of PDFAMS, which was constructed using on the Protein Data Bank (PDB) database. The alignment included acetylcholine binding proteins for which crystal structures have been obtained with ligands, notably those of *Lymnaea stagnalis* (Brejc et al., 2001; Celie et al., 2004) and *Aplysia californica* (Hansen et al., 2005). Because the crystal structures of *L. stagnalis* AChBP complexes had higher resolution (2.2 Å), the snail AChBP bound by nicotine (PDB code 1UW6) (Celie et al., 2004) was selected as the reference protein. However, imidacloprid is similar in structure to epibatidine, and the only available structure of AChBP bound by epibatidine is from *A. californica*. Therefore, the crystal structure of *A. californica* AChBP-epibatidine complex (PDB code 2BYQ) was superimposed on the structure of *L. stagnalis* AChBP bound by nicotine (PDB code 1UW6). Then imidacloprid was superimposed on the structure of epibatidine to determine the coordinates of the insecticide.

In the second step, the three-dimensional structures of α4β2 nAChR-imidacloprid complex were constructed based on the sequence and coordinates of AChBP and the coordinates of imidacloprid by the simulated annealing method (Kirkpatrick et al., 1983). The coordinates of imidacloprid were fixed during the simulated annealing. Because water molecules may play an important role for the ligand-receptor interaction, water molecules were set in the α4β2 ligand binding site at the same coordinates as those of 1UW6 (after superposition of the complex model on 1UW6). The receptor model constructed in this way was energy-minimized for 1000 iterations of conjugated gradients using the force field and partial charges of the molecular mechanics MMFF94 (Halgren 1999a,b). The structure was then subjected to molecular dynamics simulation, where it was 10 cycles of heating to 700 K and annealed slowly to 200 K. The last structure from the molecular dynamics trajectory was energy-minimized again for 1000 iterations of conjugated gradients using the force field and partial charges of MMFF94. The ligand-receptor complex with water molecules was minimized using a procedure similar to that outlined above. The model of the wild-type *D. melanogaster* Dα2/chicken β2 nAChR bound by imidacloprid was constructed in a manner similar to that used to study α4β2 nAChR-imidacloprid complex. In mutant receptor models, Thr77 and Glu79 of the β2 subunit were replaced by the mutated residues in the alignment.

Subsequent procedures were the same as employed for the wild-type proteins.

Results

In voltage-clamp electrophysiological studies, ACh and imidacloprid evoked inward currents in a dose-dependent manner in *X. laevis* oocytes expressing the wild-type and mutant $\alpha4\beta2$ and D$\alpha2\beta2$ nAChRs. The concentration-response curves for ACh and imidacloprid for the wild-type $\alpha4\beta2$ and D$\alpha2\beta2$ nAChRs, newly measured as control receptors in this study, resemble closely those previously reported (Shimomura et al., 2003, 2005). The I_{max} (normalized maximum response) and pEC_{50} [log (1/EC_{50} (M))] values of ACh for the nonmutated $\alpha4\beta2$ nAChR were 1.18 ± 0.04 and

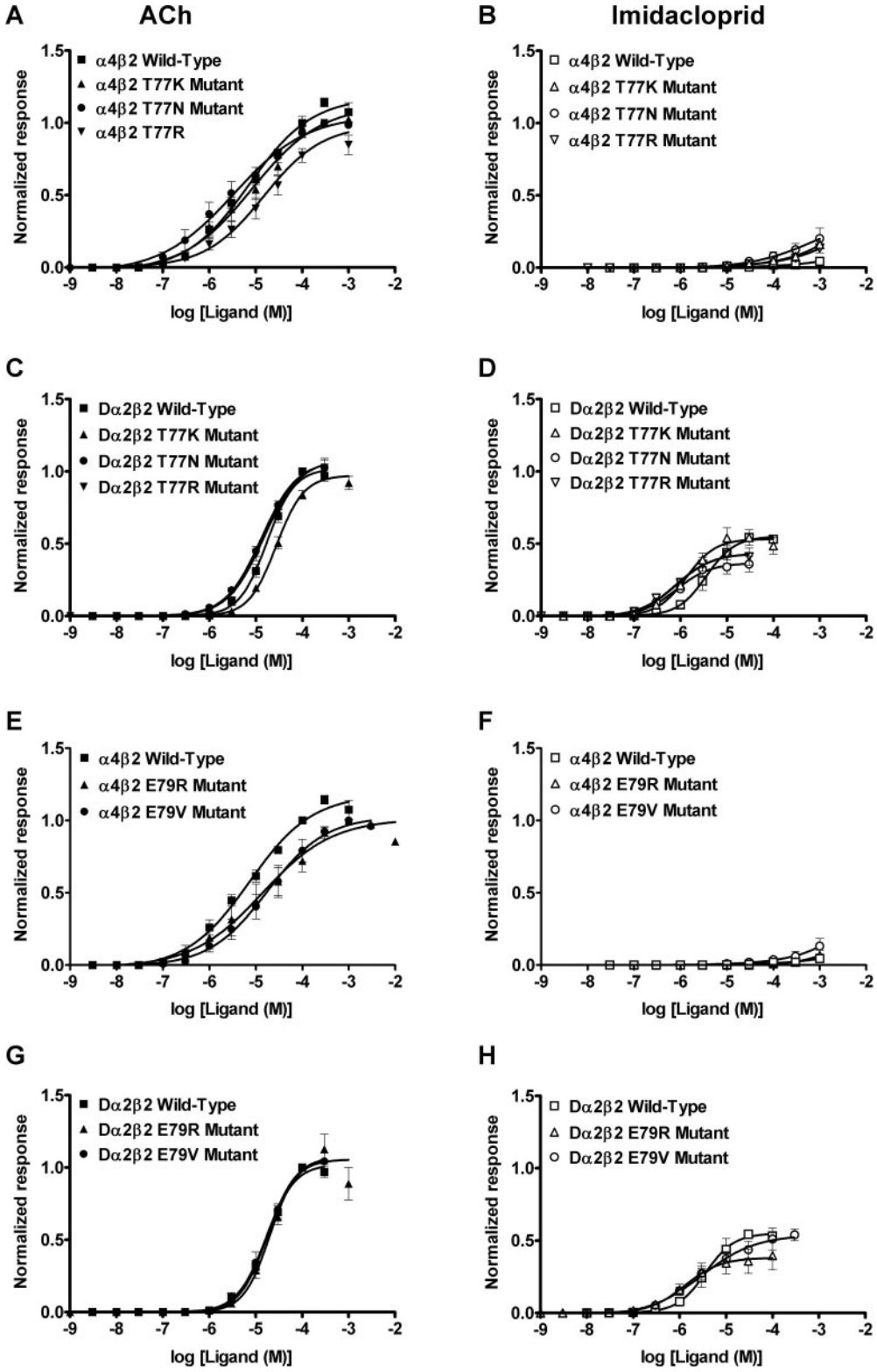

Fig. 2. Concentration-response curves of acetylcholine (ACh) (A, C, E, and G) and imidacloprid (IMI) (B, D, F, and H) obtained for wild-type, T77K, T77N, and T77R mutants of the $\alpha4\beta2$ (A and B) and D$\alpha2\beta2$ (C and D), and wild-type, E79R, and E79V mutants of the $\alpha4\beta2$ (E and F) and D$\alpha2\beta2$ (G and H) nicotinic acetylcholine receptors expressed in *X. laevis* oocytes. Each point plotted represents mean ± S.E.M. of four to eight experiments.

5.14 ± 0.07 (n = 7), respectively, whereas the I_{max} and pEC_{50} values for the wild-type Dα2β2 nAChR were 1.02 ± 0.02 and 4.76 ± 0.03 (n = 7), respectively (Fig. 2, Table 2). The responses to imidacloprid of the wild-type α4β2 nAChR were too small to obtain the I_{max} and pEC_{50} values, whereas imidacloprid activated the wild-type Dα2β2 nAChR with I_{max} and pEC_{50} values of 0.55 ± 0.03 and 5.45 ± 0.08 (n = 4), respectively (Fig. 2, Table 2).

The pEC_{50} value of ACh for the α4β2 nAChR was minimally shifted by T77K [5.08 ± 0.13 (n = 5)], T77N [5.47 ± 0.12 (n = 5)], T77R [4.83 ± 0.12 (n = 6)], E79R [4.86 ± 0.16 (n = 4)], and E79V [4.76 ± 0.05 (n = 4)] mutations (Fig. 2, A and E; Table 2). Likewise, imidacloprid failed to activate the α4β2 nAChR irrespective of the presence or absence of such single amino acid replacements in loop D (Fig. 2, B and F, Table 2).

When Thr77 in loop D of the β2 subunit was replaced by lysine in the Dα2β2 nAChR, the ACh concentration-response curve was shifted to the right [pEC_{50} = 4.56 ± 0.03 (n = 6)] (Fig. 2C, Table 2). However, this was unique, and all other changes in the concentration-response curve of ACh for the Dα2β2 nAChR after a single amino acid mutation at position of 77 or 79 in loop D of the β2 subunit were minimal: Dα2β2 (T77N) mutant, 4.88 ± 0.04 (n = 5); Dα2β2 (T77R) mutant, 4.83 ± 0.04 (n = 5); Dα2β2 (E79R) mutant, 4.70 ± 0.05 (n = 5); Dα2β2 (E79V) mutant, 4.75 ± 0.04 (n = 6) (Fig. 2, C and G, Table 2). On the other hand, T77N or T77R mutation in loop D of the β2 subunit resulted in significant shifts of the imidacloprid concentration-response curve to the left [pEC_{50} values of imidacloprid for the T77N and T77R mutants of Dα2β2 nAChR were 6.10 ± 0.12 (n = 4) and 6.11 ± 0.12 (n = 7), respectively] (Fig. 2D, Table 2). In all other cases, the concentration-response curves for the Dα2β2 nAChR of imidacloprid resulting from single amino acid replacements were similar to those observed for Dα2β2 wild-type nAChR (Fig. 2, D and H, Table 2).

To help interpret these results, three-dimensional models of the ligand binding site of the α4β2 and Dα2β2 nAChRs bound by imidacloprid were constructed (Fig. 3). The wild-type models (Fig. 3, A and B) show Thr77 in proximity to the nitro group of imidacloprid. Comparing α4β2 and Dα2β2 nAChR models indicates stronger contact with the nitro group of the insecticide in the case of the hybrid Dα2β2 nAChR. In both cases, Glu79 seems to indirectly influence the interactions of Thr77. Thus, mutation of Thr77 and Glu79 is predicted to influence imidacloprid interactions with both nAChRs under investigation. Fig. 3, C and D, show that T77R;E79V double mutations in the α4β2 and Dα2β2 nAChRs can assist in the electrostatic interactions of the basic residue with the nitro group of imidacloprid, thereby enhancing markedly agonist affinity. Therefore, we have also investigated the effects of combined mutations of Thr77 and Glu79 in loop D to residues observed in the insect non-α subunits on the responses to imidacloprid of the α4β2 and Dα2β2 nAChRs.

Compared with the effects of the single amino acid mutations, the effects of double amino acid mutations at positions 77 and 79 were striking. The T77R;E79V double mutant of the α4β2 nAChR showed greatly enhanced responses to imidacloprid (Fig. 4, A and B). The pEC_{50} and I_{max} values of imidacloprid for the α4β2 (T77K;E79R) mutant were 4.50 ± 0.18 and 0.53 ± 0.06 (n = 6), respectively (Table 2).

The T77K;E79R, T77N;E79R, and T77R;E79V mutations of the Dα2β2 nAChR shifted the imidacloprid concentration-response curve dramatically to the left (Figs. 4, C and D, and 5D). The pEC_{50} values of imidacloprid for the T77K;E79R, T77N;E79R, and T77R;E79V mutants were 5.87 ± 0.07, 6.58 ± 0.06, and 6.19 ± 0.12, respectively (Table 2). The I_{max} values obtained from the dose-response curve of imidacloprid for the T77K;E79R, T77N;E79R, and T77R;E79V mutants were 0.63 ± 0.03 (n = 5), 0.65 ± 0.02 (n = 6), and 0.44 ± 0.03 (n = 8), respectively (Table 2). By contrast, for both receptor

TABLE 2

I_{max}, EC_{50}, and n_H values of acetylcholine and imidacloprid for wild-type and mutant α4β2 and Dα2β2 nicotinic acetylcholine receptors

Values shown are the result of a fit of the concentration-response data (mean ± S.E.M., 4–8) illustrated in Figs. 2 or 4. Statistical test (one-way ANOVA, Dunnett's multiple-comparison test) is for significant differences from the wild-type data

	Acetylcholine			Imidacloprid		
	I_{max}	pEC_{50}	n_H	I_{max}	pEC_{50}	n_H
α4β2 Wild-type	1.18 ± 0.04	5.14 ± 0.07	0.6 ± 0.1	N.D.	N.D.	N.D.
	1.17 ± 0.05[a]	5.12 ± 0.09[a]	0.6 ± 0.1[a]	N.D.[a]	N.D.[a]	N.D.[a]
α4β2 T77K	1.12 ± 0.07	5.08 ± 0.13	0.6 ± 0.1	N.D.	N.D.	N.D.
α4β2 T77N	1.06 ± 0.06	5.47 ± 0.12	0.6 ± 0.1	N.D.	N.D.	N.D.
α4β2 T77R	0.99 ± 0.06*	4.83 ± 0.13	0.7 ± 0.1	N.D.	N.D.	N.D.
α4β2 E79R	1.01 ± 0.07	4.86 ± 0.16	0.6 ± 0.1	N.D.	N.D.	N.D.
α4β2 E79V	1.03 ± 0.05	4.76 ± 0.10	0.7 ± 0.1	N.D.	N.D.	N.D.
α4β2 T77K;E79R	1.09 ± 0.03	4.52 ± 0.06**	0.9 ± 0.1	0.07 ± 0.02	3.67 ± 0.25	1.4 ± 0.8
α4β2 T77N;E79R	1.00 ± 0.04	5.02 ± 0.08	0.9 ± 0.1	N.D.	N.D.	N.D.
α4β2 T77R;E79V	1.02 ± 0.04	5.39 ± 0.08	0.8 ± 0.1	0.53 ± 0.06	4.50 ± 0.18	0.9 ± 0.3
Dα2β2 Wild-type	1.02 ± 0.02	4.76 ± 0.03	1.5 ± 0.1	0.55 ± 0.03	5.45 ± 0.08	1.4 ± 0.3
	1.00 ± 0.03[a]	4.81 ± 0.05[a]	1.5 ± 0.2[a]	0.62 ± 0.02[a]	5.83 ± 0.05[a]	1.7 ± 0.3[a]
Dα2β2 T77K	0.97 ± 0.02	4.56 ± 0.03**	1.5 ± 0.1	0.53 ± 0.03	5.88 ± 0.08	1.4 ± 0.3
Dα2β2 T77N	1.07 ± 0.03	4.88 ± 0.04	1.1 ± 0.1	0.37 ± 0.03*	6.10 ± 0.12*	1.2 ± 0.3
Dα2β2 T77R	1.08 ± 0.03	4.83 ± 0.04	1.1 ± 0.1	0.43 ± 0.03	6.11 ± 0.12**	1.1 ± 0.3
Dα2β2 E79R	1.06 ± 0.04	4.70 ± 0.05	1.5 ± 0.2	0.38 ± 0.04*	5.89 ± 0.16	1.1 ± 0.4
Dα2β2 E79V	1.08 ± 0.03	4.75 ± 0.04	1.4 ± 0.1	0.54 ± 0.05	5.52 ± 0.15	0.8 ± 0.2
Dα2β2 T77K;E79R	0.96 ± 0.02	4.19 ± 0.03**	1.8 ± 0.2	0.63 ± 0.03	5.87 ± 0.07	1.3 ± 0.3
Dα2β2 T77N;E79R	1.09 ± 0.03	4.67 ± 0.04	1.4 ± 0.1	0.65 ± 0.02	6.58 ± 0.06**	1.5 ± 0.2
Dα2β2 T77R;E79V	1.00 ± 0.03	4.49 ± 0.05**	1.3 ± 0.2	0.44 ± 0.03	6.19 ± 0.12**	1.0 ± 0.3

N.D., not determined because the concentration-response curve did not plateau even at 1 mM.
* $P < 0.05$; ** $P < 0.01$.
[a] Data are from Shimomura et al. (2005).

types, the dose-response curves for ACh were much less affected by the double mutations in loop D of the β2 subunit (Fig. 5, A and C, Table 2).

Discussion

In this study, we have shown that amino acid substitutions in loop D designed to mimic insect non-α subunits greatly increase the affinity of imidacloprid in terms of the pEC_{50} value for the $\alpha4\beta2$ and D$\alpha2\beta2$ nAChRs, whereas the impact on ACh concentration-response curve is much smaller. This points to an important role for loop D in the selectivity of imidacloprid for the recombinant nAChRs investigated.

To enhance significantly the imidacloprid-sensitivity of the $\alpha4\beta2$ nAChR in terms of the shift of pEC_{50} value, it was necessary to replace not only Thr77 by a basic residue, but also Glu79 by the neutral residue valine. An interpretation of this result is that the electrostatic force of Arg77 enhancing the $\alpha4\beta2$ nAChR-imidacloprid interactions is suppressed by the negative electrostatic force of Glu79 only when the T77R mutation was added to loop D. However, this "lock" is removed by the E79V mutation, resulting in an enhancement of the current amplitudes in response to imidacloprid. The shift of the imidacloprid concentration-response curve for the $\alpha4\beta2$ and D$\alpha2\beta2$ nAChRs by the T77K;E79R double mutation was smaller than that induced by the T77R;E79V double mutation. In view of the result that the ACh concentration-response curves were shifted by the T77K;E79R mutation to higher concentrations irrespective of the kinds of nAChRs tested (Table 2), this mutation might alter the conformation of the agonist binding site to reduce the affinity of all agonists, thereby counteracting the enhancement of the affinity for imidacloprid by the basic residues.

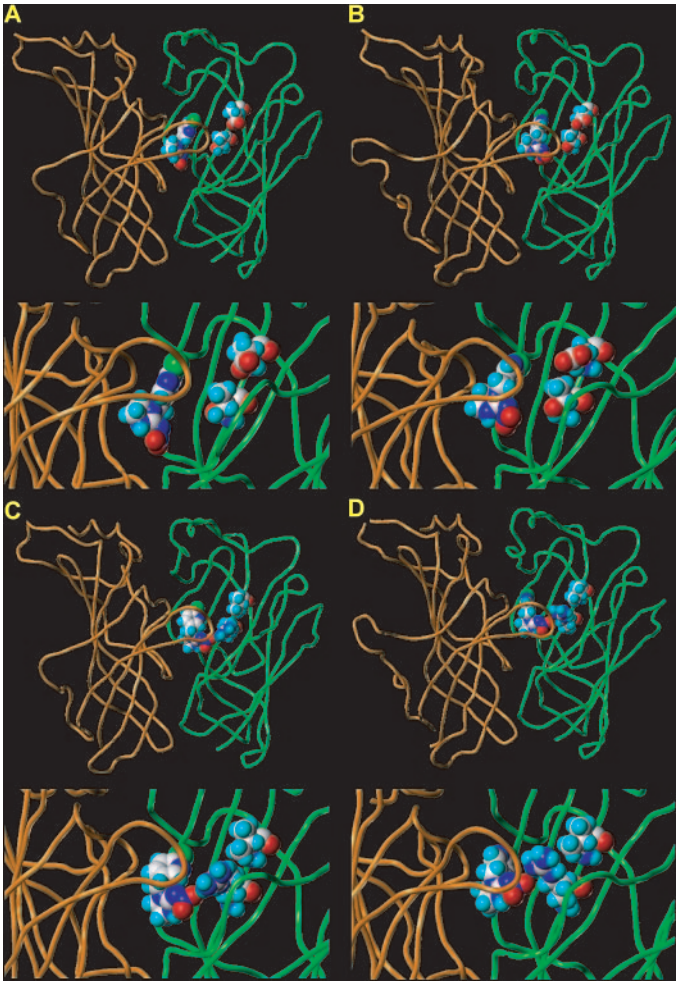

Fig. 3. Homology models of the agonist binding domain of the wild-type $\alpha4\beta2$ (A) and D$\alpha2\beta2$ (B) nAChRs and their T77R;E79V mutants (C, $\alpha4\beta2$ nAChR; D, D$\alpha2\beta2$ nAChRs) bound by imidacloprid constructed using the crystal structures of the AChBP from *L. stragnalis* (PDB code 1UW6) and *A. californica* (PDB code 2BYQ). The figures were made using Sybyl version 6.91 and PDFAMS (see *Materials and Methods* for details). In the wild-type nAChR models, only imidacloprid, Thr77, and Glu79 are shown by the space-filling model, whereas in the mutant nAChR models, only imidacloprid, Arg77, and V79 are shown (main chain of the $\alpha4$ and D$\alpha2$ subunits, orange; main chain of the $\beta2$ subunit, green; carbon, white; hydrogen, cyan; nitrogen, blue; oxygen, red; chlorine, green blue). Enlarged views are shown under respective whole views.

We have generated three-dimensional models of wild-type and mutant $\alpha4\beta2$ and D$\alpha2\beta2$ nAChRs bound by imidacloprid to help understand the mechanism underlying the results of the site-directed mutagenesis (Fig. 3). The locations of key amino acid residues [Tyr121 (loop A), Trp177 (loop B), Tyr218 (loop C), Cys220 (loop C), Cys221 (loop C), and Tyr225 (loop C) of the $\alpha4$ subunit; and Trp75 (loop D) and Phe137 (loop E) of the $\beta2$ subunit; residue numbering is from the start methionine] in the models resemble those located in the model reported previously by Le Novère et al. (2002). The nitro group seems to be located apart from Thr77 in the wild-type $\alpha4\beta2$ nAChR model (Fig. 3A), whereas the nitro group oxygens make contact with Arg77 in the T77R;E79V mutant model (Fig. 3C), consistent with the shift to lower concentrations of the imidacloprid concentration-response curve after the T77R;E79V double mutation (Figs. 4 and 5). Likewise, the T77R;E79V double mutation, which resulted in a significant decrease of the EC_{50} value of imidacloprid for the D$\alpha2\beta2$ hybrid nAChR (Figs. 4 and 5), placed the nitro group in contact with Arg77 in the model (Fig. 3D). Thus, the enhancement of the recombinant AChRs after the double site-directed mutagenesis is probably due to direct electrostatic interactions of the nitro group of imidacloprid with the basic residues in loop D.

The D$\alpha2\beta2$ hybrid nAChR was more sensitive to imidacloprid than the $\alpha4\beta2$ nAChR in terms of the shift of the imidacloprid concentration-response curve, suggesting that the D$\alpha2$ subunit possesses structural features favoring interactions with imidacloprid. This agrees well with earlier findings that the region upstream of loop B and an amino acid in loop C also play a role in determining selectivity (Shimomura et al., 2004a, 2005). However, the contribution of the non-α subunit $\beta2$ to the interactions with imidacloprid should not be undervalued, as demonstrated earlier by Lansdell and Millar (2000). The molecular modeling (Fig. 3B) showed closer proximity of the nitro group to Thr77 in the D$\alpha2\beta2$ nAChR compared with its position in the $\alpha4\beta2$ nAChR (Fig. 3A), thereby facilitating hydrogen bond formation between the ligand and the hybrid nAChR. Consistent with the models, not only T77N;E79R and T77R;E79V double mutations but also T77N and T77R point mutations significantly increased the pEC_{50} value of imidacloprid in the D$\alpha2\beta2$ nAChR, which was not observed for the $\alpha4\beta2$ nAChR. All these results seem to suggest that the amino acids newly introduced to position 77 in loop D are able to interact more strongly with the nitro group of imidacloprid in the D$\alpha2\beta2$ nAChR than in the $\alpha4\beta2$ nAChR, thereby resulting in the

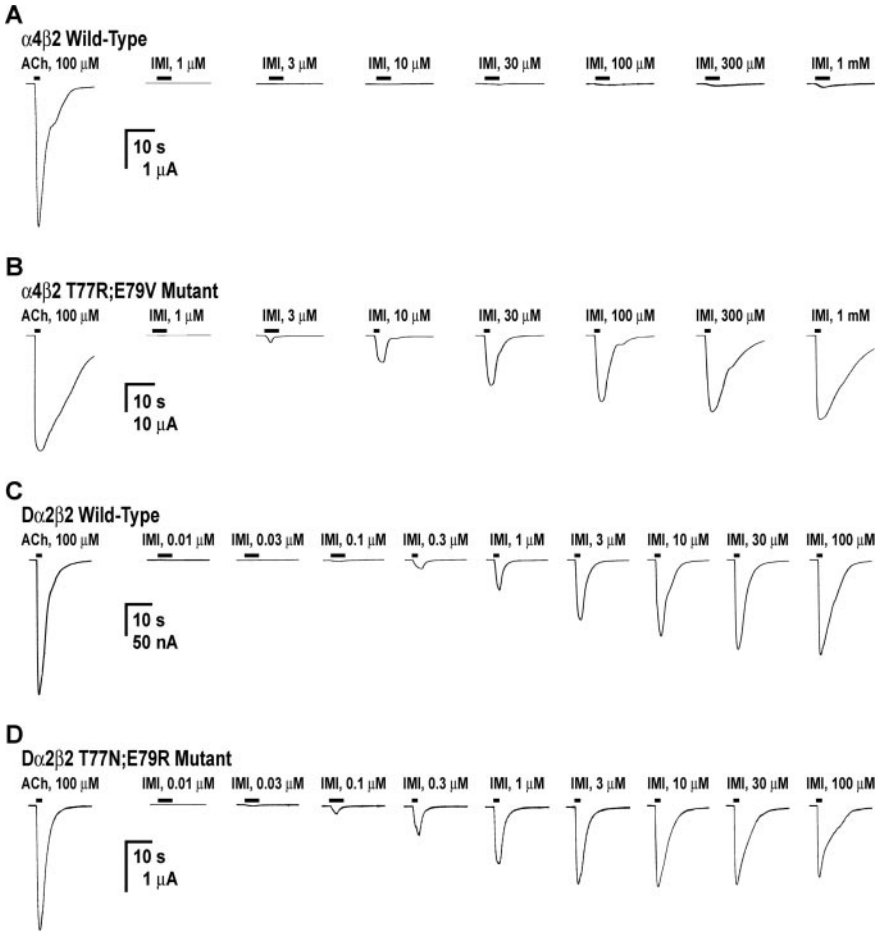

Fig. 4. Inward currents recorded using two electrode voltage-clamp electrophysiology in response to bath-applied acetylcholine (ACh) and imidacloprid (IMI) of the wild-type $\alpha 4\beta 2$ nicotinic acetylcholine receptor (nAChR) (A) and its T77R;E79V mutant (B) and the wild-type $D\alpha 2\beta 2$ nAChR (C) and its T77N;E79R mutant (D) expressed in *X. laevis* oocytes.

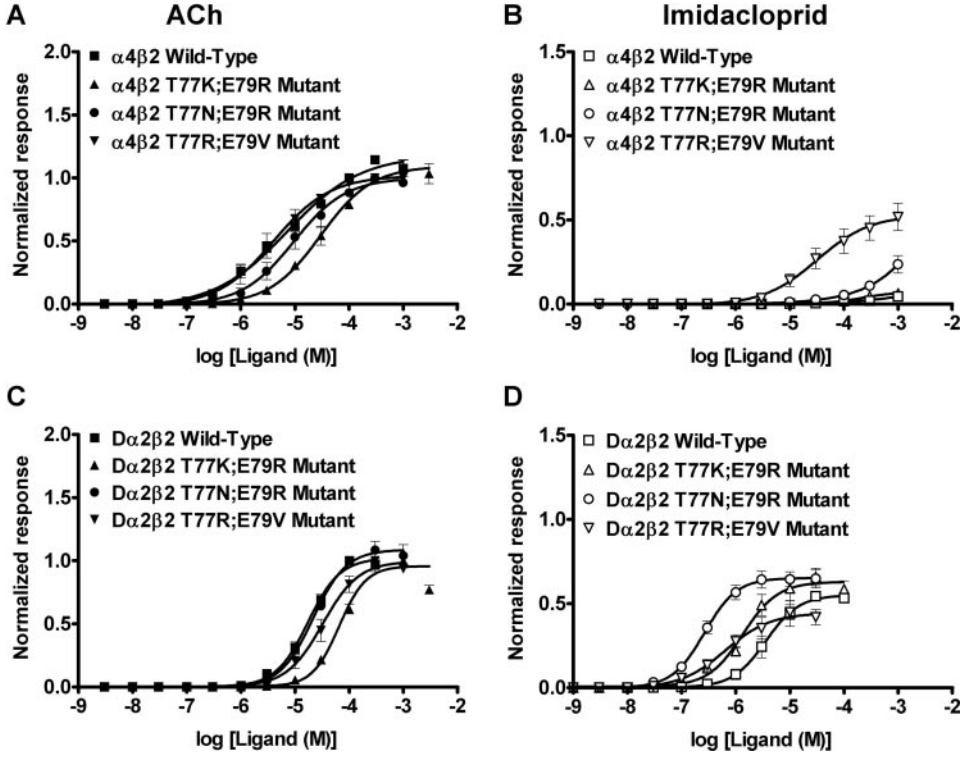

Fig. 5. Concentration-response curves of acetylcholine (ACh) (A and C) and imidacloprid (IMI) (B and D) obtained for wild-type, T77K;E79R, T77N;E79R, and T77R;E79V mutants of the $\alpha 4\beta 2$ (A and B) and $D\alpha 2\beta 2$ (C and D) nicotinic acetylcholine receptors expressed in *X. laevis* oocytes. Each point plotted represents mean ± S.E.M. of four to eight experiments

significant shifts of the imidacloprid concentration-response curve to lower concentrations (Table 2). However, the high imidacloprid sensitivity of the Dα2β2 nAChR may stem partly from the interactions of one of the two nitro group oxygens with other regions than loop D. Thus, further studies are necessary to fully understand the mechanism for the selectivity of neonicotinoids.

The EC_{50} value of imidacloprid in the T77N;E79R mutant of the Dα2β2 nAChR is lower than 1 μM, which is close to the value determined for native nAChRs on the cockroach (*Periplaneta americana*) native neurons (Ihara et al., 2006). Therefore, the overall difference in imidacloprid sensitivity between insect and mammalian nAChRs in vivo can be accounted for by the interactions with loop D in the non-α subunit combined with those with loop C and the region upstream of loop B in the α subunit of insect nAChRs (Shimomura et al., 2004a, 2005).

In conclusion, we have shown that the basic residues observed only in insect nAChR loop D play a key role in the selective interactions of heteromeric nAChRs with neonicotinoids. It is conceivable that the double mutations in loop D enhance markedly the imidacloprid sensitivity of not only α4β2 and Dα2β2 nAChRs tested in this study, but also other nAChRs. Molecular modeling has been employed, based on the structure of AChBP with nicotine bound, and this accounts well for the experimental data obtained by site-directed mutagenesis. It has been found recently that a mutation in loop B leads to a neonicotinoid resistance in brown leaf hoppers (Liu et al., 2005). In the future, the model developed here could be exploited further to examine the molecular basis of neonicotinoid resistance and to study the docking of newly developed insecticide candidates with nAChRs. In the context of receptor-based neonicotinoid resistance, our findings indicate that substitutions to nonbasic residues in two key sites in loop D may also lead to a neonicotinoid resistant phenotype because the effects of such structural changes on the ACh concentration-response curve are minimal. The present study contributes to our understanding of the molecular mechanism underlying selectivity of neonicotinoids and suggests a possible target region on which to focus in the design of new insecticides.

References

Azam L, Winzer-Serhan U, and Leslie FM (2003) Co-expression of α7 and β2 nicotinic acetylcholine receptor subunit mRNAs within rat brain cholinergic neurons. *Neuroscience* **119:**965–977.

Bertrand D, Ballivet M, Gomez M, Bertrand S, Phannavong B, and Gundelfinger ED (1994) Physiological properties of neuronal nicotinic receptors reconstituted from the vertebrate β2 subunit and *Drosophila* α subunits. *Eur J Neurosci* **6:**869–875.

Brejc K, van Dijk WJ, Klaassen RV, Schuurmans M, van Der Oost J, Smit AB, and Sixma TK (2001) Crystal structure of an ACh-binding protein reveals the ligand-binding domain of nicotinic receptors. *Nature (Lond)* **411:**269–276.

Celie PHN, van Rossum-Fikkert SE, van Dijk WJ, Brejc K, Smit AB, and Sixma TK (2004) Nicotine and carbamylcholine binding to nicotinic acetylcholine receptors as studied in AChBP crystal structures. *Neuron* **41:**841–842.

Corringer P-J, Le Novère N, and Changeux J-P (2000) Nicotinic receptors at the amino acid level. *Annu Rev Pharmacol Toxicol* **40:**431–458.

Couturier S, Bertrand D, Matter J-M, Hernandez M-C, Bertrand S, Millar N, Valera S, Barkas T, and Ballivet M (1990) A neuronal nicotinic acetylcholine receptor subunit (α7) is developmentally regulated and forms a homo-oligomeric channel blocked by α-BTX. *Neuron* **5:**847–856.

Deglise P, Grunewald B, and Gauthier M (2002) The insecticide imidacloprid is a partial agonist of the nicotinic receptor of honeybee Kenyon cells. *Neurosci Lett* **321:**13–16.

Elgoyhen AB, Johnson DS, Boulter J, Vetter DE, and Heinemann S (1994) α9: An acetylcholine receptor with novel pharmacological properties expressed in rat cochlear hair cells. *Cell* **79:**705–715.

Elgoyhen AB, Vetter DE, Katz E, Rothlin CV, Heinemann SF, and Boulter J (2001) α10: a determinant of nicotinic cholinergic receptor function in mammalian vestibular and cochlear mechanosensory hair cells. *Proc Natl Acad Sci USA* **98:**3501–3506.

Gepner JI, Hall LM, and Sattelle DB (1978) Insect acetylcholine receptors as a site of insecticide action. *Nature (Lond)* **276:**188–190.

Gerzanich V, Anand R, and Lindstrom J (1994) Homomers of α8 and α7 subunits of nicotinic receptors exhibit similar channel but contrasting binding site properties. *Mol Pharmacol* **45:**212–220.

Halgren TA (1999a) MMFF VI. MMFF94s option for energy minimization studies. *J Comput Chem* **20:**720–729.

Halgren TA (1999b) MMFF VII. Characterization of MMFF94, MMFF94s, and other widely available force fields for conformational energies and for intermolecular-interaction energies and geometries. *J Comput Chem* **20:**730–748.

Hansen SB, Sulzenbacher G, Huxford T, Marchot P, Taylor P, and Bourne Y (2005) Structures of *Aplysia* AChBP complexes with nicotinic agonists and antagonists reveal distinctive binding interfaces and conformations. *EMBO (Eur Mol Biol Organ) J* **24:**3635–3646.

Ihara M, Brown LA, Ishida C, Okuda H, Sattelle DB, and Matsuda (2006) Actions of imidacloprid, clothianidin and related neonicotinoids on nicotinic acetylcholine receptors of American cockroach neurons and their relationships with insecticidal potency. *J Pestic Sci* **31:**35–40.

Ihara M, Matsuda K, Otake M, Kuwamura M, Shimomura M, Komai K, Akamatsu M, Raymond V, and Sattelle DB (2003) Diverse actions of neonicotinoids on chicken α7, α4β2 and *Drosophila*-chicken SADβ2 and ALSβ2 hybrid nicotinic acetylcholine receptors expressed *Xenopus laevis* oocytes. *Neuropharmacology* **45:**133–144.

Ihara M, Matsuda K, Shimomura M, Sattelle DB, and Komai K (2004) Super agonist action of clothianidin and related compounds on SADβ2 nicotinic acetylcholine receptor expressed in *Xenopus laevis* oocytes. *Biosci Biotechnol Biochem* **68:**761–763.

Karlin A (2002) Emerging structure of the nicotinic acetylcholine receptors. *Nat Rev Neurosci* **3:**102–114.

Kirkpatrick S, Gelatt CD, and Vecchi MP (1983) Optimization by simulated annealing. *Science (Wash DC)* **220:**671–680.

Lansdell SJ and Millar NS (2000) The influence of nicotinic receptor subunit composition upon agonist, α-bungarotoxin and insecticide (imidacloprid) binding affinity. *Neuropharmacology* **39:**671–679.

Le Novère N, Grutter T, and Changeux J-P (2002) Models of the extracellular domain of the nicotinic receptors and of agonist- and Ca^{2+}-binding sites. *Proc Natl Acad Sci USA* **99:**3210–3215.

Lindstrom JM (2003) Nicotinic acetylcholine receptors of muscles and nerves: comparison of their structures, functional roles, and vulnerability to pathology. *Ann NY Acad Sci* **998:**41–52.

Liu Z, Williamson MS, Lansdell SJ, Denholm I, Han Z, and Millar NS (2005) A nicotinic acetylcholine receptor mutation conferring target-site resistance to imidacloprid in *Nilaparvata lugens* (brown planthopper). *Proc Natl Acad USA* **102:**8420–8425.

Matsuda K, Buckingham SD, Freeman JC, Squire MD, Baylis HA, and Sattelle DB (1998) Effect of the α subunit on imidacloprid sensitivity of recombinant nicotinic acetylcholine receptors. *Br J Pharmacol* **123:**518–524.

Matsuda K, Buckingham SD, Kleier D, Rauh JJ, Grauso M, and Sattelle DB (2001) Neonicotinoids: insecticides acting on insect nicotinic acetylcholine receptors. *Trends Pharmacol Sci* **22:**573–580.

Matsuda K, Shimomura M, Ihara M, Akamatsu M, and Sattelle DB (2005) Neonicotinoids show selective and diverse actions on their nicotinic receptor targets: Electrophysiology, molecular biology, and receptor modeling studies. *Biosci Biotechnol Biochem* **69:**1442–1452.

Matsuda K, Shimomura M, Kondo Y, Hashigmi K, Yoshida N, Raymond V, Mongan NP, Freeman JC, Komai K, and Sattelle DB (2000) Role of loop D of the α7 nicotinic acetylcholine receptor in its insecticide imidacloprid and related neonicotinoids. *Br J Pharmacol* **130:**981–986.

Mencke N and Jeschke P (2002) Therapy and prevention of parasitic insects in veterinary medicine using imidacloprid. *Curr Top Med Chem* **2:**701–715.

Moriya K, Shibuya K, Hattori Y, Tsuboi S, Shiokawa K, and Kagabu S (1992) 1-(6-Chloronicotinyl)-2-nitroimino-imidazolidines and related compounds as potential new insecticides. *Biosci Biotechnol Biochem* **56:**364–365.

Nagata K, Aistrup GL, Song JH, and Narahashi T (1996) Subconductance-state currents generated by imidacloprid at the nicotinic acetylcholine receptor in PC 12 cells. *Neuroreport* **7:**1025–1028.

Ogata K and Umeyama H (2000) An automatic homology modeling method consisting of database searches and simulated. *J Mol Graph Model* **18:**258–272.

Palma E, Maggi L, Barabino B, Eusebi F, and Ballivet M (1999) Nicotinic acetylcholine receptors assembled from the α7 and β3 subunits. *J Biol Chem* **274:**18335–18340.

Rust MK (2005) Advances in the control of *Ctenocephalides felis* (cat flea) on cats and dogs. *Trends Parasitol* **21:**232–236.

Salgado VL and Saar R (2004) Desensitizing and non-desensitizing subtypes of α-bungarotoxin-sensitive nicotinic acetylcholine receptors in cockroach neurons. *J Insect Physiol* **50:**867–879.

Sattelle DB (1980) Acetylcholine receptors of insects. *Adv Insect Physiol* **15:**115–215.

Sattelle DB and Breer H (1990) Cholinergic nerve terminals in the central nervous system of insects: molecular aspects of structure, function and regulation. *J Neuroendocrinol* **2:**241–156.

Shimomura M, Matsuda K, Akamatsu M, Sattelle DB, and Komai K (2004b) Effects of mutations of isoleucine 191 in loop F to aromatic residues on the responses to neonicotinoids of chicken α7 nicotinic acetylcholine receptor. *J Pestic Sci* **29:**364–368.

Shimomura M, Okuda H, Matsuda K, Komai K, Akamatsu M, and Sattelle DB (2002) Effects of mutations of a glutamine residue in loop D of the α7 nicotinic acetylcholine receptor on agonist profiles for neonicotinoid insecticides and related ligands. *Br J Pharmacol* **137:**162–169.

Shimomura M, Satoh H, Yokota M, Ihara M, Matsuda K, and Sattelle DB (2005) Insect-vertebrate chimeric nicotinic acetylcholine receptors identify a region N-terminal to loop B of the *Drosophila* Dα2 subunit which contributes to neonicotinoid sensitivity. *Neurosci Lett* **385:**168–172.

Shimomura M, Yokota M, Matsuda K, Sattelle DB, and Komai K (2004a) Roles of loop C and the loop B-C interval of the nicotinic receptor a subunits in its selective interactions with imidacloprid in insects. *Neurosci Lett* **363:**195–198.

Shimomura M, Yokota M, Okumura M, Matsuda K, Akamatsu M, Sattelle DB, and Komai K (2003) Combinatorial mutations in loops D and F strongly influence responses of the α7 nicotinic acetylcholine receptor to imidacloprid. *Brain Res* **991:**71–77.

Swick AG, Janicot M, Chenval-Kastlic T, McLenithan JC, and Lane MD (1992) Promoter-cDNA-directed heterologous protein expression in *Xenopus laevis* oocytes. *Proc Natl Acad Sci USA* **89:**1812–1816.

Tomizawa M and Casida JE (2005) Neonicotinoid insecticide toxicology: mechanisms of selective action. *Annu Rev Pharmacol Toxicol* **45:**247–268.

Tomizawa M, Lee DL, and Casida JE (2003) Selective toxicity of neonicotinoids attributable to specificity of insect and mammalian nicotinic receptors. *Annu Rev Entomol* **48:**339–364.

Address correspondence to: Kazuhiko Matsuda PhD, Department of Applied Biological Chemistry, School of Agriculture, Kinki University, 3327–204 Nakamachi, Nara 631-8505, Japan. Email: kmatsuda@nara.kindai.ac.jp